[8] Etching of silicon dioxide in off-electrode plasma using a chrome mask

V.V. Podlipnov [1, 2], V.A. Kolpakov [2], N.L. Kazanskiy [1, 2]
[1] Image Processing Systems Institute of RAS – Branch of the FSRC "Crystallography and Photonics" of RAS, Samara, Russia,
[2] Samara National Research University, Samara, Russia

Abstract

We discuss results of etching a Cr-SiO_2 structure in a flow of off-electrode gas-discharge plasma in a CF_4 + O_2 gas at a ratio of 50:1, at the discharge current I = 80 mA, accelerating voltage U = 1.2 kV, and process duration t = 5 min. It was shown that changes in the intensity of Raman spectral bands in the course of etching correspond to nanoscale changes in the thin Cr-SiO_2 films and a chrome mask. The peculiarity of the etching process consists in the removal of the Cr_2O_3 oxide with increasing amount of nitrogen molecules in the structure of the Cr film. It was found that spray products deposited inside the chrome mask windows at U = 1.2 kV and I = 80 mA are in the form of Cr_2N, according to their Raman spectra.

Keywords: *diffusion, ion-electron beam, etch, reprecipitation, micromasking.*

Citation: *Podlipnov VV, Kolpakov VA, Kazanskiy NL. Etching of silicon dioxide in off-electrode plasma using a chrome mask. Computer Optics 2016; 40(6): 830-836.*

DOI: 10.18287/2412-6179-2016-40-6-830-836.

Introduction

Plasma etching is widely used in microelectronics and diffractive optics processes during microrelief formation on semiconductor and dielectric substrates, since it permits to attain high quality of obtained elements [1]. Formerly in papers [2 – 7], the authors showed research perspectives for different applications of off-electrode gas-discharge plasma in microrelief formation processes in diffractive optical elements (DOEs).

Thin metal mask films became widespread in DOE microrelief formation processes using chemical plasma etching techniques [8 – 10]. During optical material etching processes, these masks permit achieving high etching selectivity of semiconductor and dielectric materials versus metals. Besides, it is possible for various metals to form a certain topology using a method of direct laser ablation without additional lithographic processes that is especially useful and may partly reduce the cost of production of large-aperture DOEs [11]. The analysis of thermo-chemical laser recording processes enabled us to significantly improve resolution power in masking processes [12 – 13]. A combination of the above masking and off-electrode plasma etching techniques can significantly reduce the cost of production and increase the production rate of large-aperture diffractive optical elements. However, no special attention was previously given to the study of peculiarities of silicon dioxide etching techniques in off-electrode plasma using thin metal mask films, as well as to the influence of this plasma on properties and structure of the above mentioned films. And this is the reason why this paper presents research results referring to the influence of off-electrode plasma on properties and structure of chrome mask layers depending on operation modes of a gas-discharge device.

1. Experimental procedures

Fused quartz substrates (quartz grade KV), 25 mm in diameter and 3 mm thick with the original roughness R_a = 3 – 5 nm, were selected as blank substrates. Before being sprayed, the substrates went through chemical cleaning in concentrated alkaline solution of potassium hydroxide, then in solution of potassium bichromate and concentrated sulfuric acid at a temperature of 45 – 50°C, and then they were subjected to flushing in deionized water with specific resistivity of at least18 MOm/cm. The substrates were placed into a vacuum chamber of a pulse current magnetron sputterer Carolina D-12A where the surfaces were subjected to adsorbed-gas ion-beam cleaning with the purpose of additional puri-

fication. A layer of Cr 40 – 60 nm in thickness was applied on the surface of the substrates. Automatic film-thickness deposition control was carried out with the help of a quartz thickness gauge. For better adhesion quality, the substrate temperature was maintained at a level of 200°C. The utilized capacity of the magnetron sputterer was 0.8 kW in an atmosphere of high pure argon plasma-forming gas. A gas flow into the vacuum chamber was maintained at a level of 3 l/h. In order to avoid the influence of laser effects on properties of chrome films, the microrelief topology of test structures was formed by means of electron lithography using a scanning electron microscope (SEM) Carl Zeiss Supra 25 equipped with a nanolithography tool Xenos Xedraw 2 [14]. An electron-beam resist layer (ERP-40) 500 nm in thickness was applied on the surface of chromium by centrifuging. Rectangular windows 30×70 µm in size were formed in order to create test structures for the purpose of optimization of etching processes in a resistive layer. Liquid etching of a chrome layer was performed in cerium (IV) sulphate tetrahydrate solution using the above mentioned mask. A metal mask shown in Fig. 1was obtained chemically on the surface of the fused quart after removing the resistive mask.

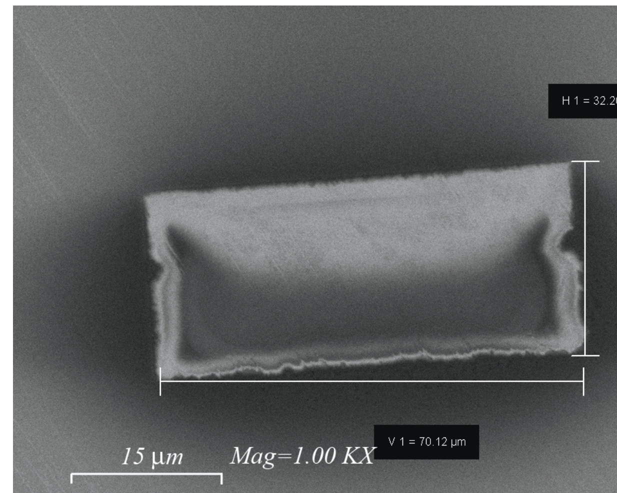

Fig. 1. The metal mask

Using the above mentioned mask, plasma-chemical etching of silicon dioxide was performed in off-electrode plasma in the following modes: I = 50 mA, U = 1200 V and I = 80 mA, U = 2000 V, respectively. The process time was 5 minutes in both cases. The gas-discharge device was used as a source of off-electrode plasma. Its design is described in detail in paper [15]. Installation diagram of an experimental plant is shown in Fig. 2.

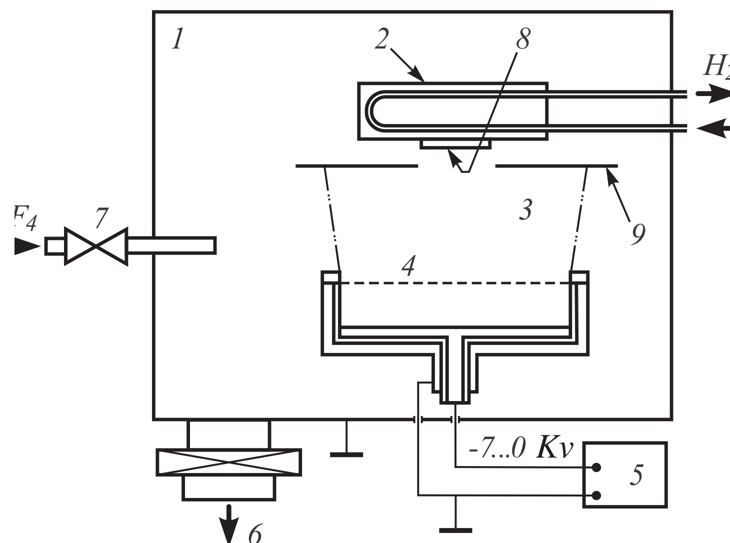

Fig. 2. Installation diagram of the experimental plant for microstructure etching: 1 – the vacuum chamber, 2 – a water-cooled substrate holder, 3 – a low-temperature plasma-forming region, 4 – a large-aperture source of off-electrode plasma, 5 – a high-voltage power supply, 6 – a discharge system, 7 – a plasma-forming gas puffing system, 8 – the substrate, 9 – a screen

The test samples 8 (Fig. 2) were placed in the vacuum chamber (1) and fixed on the water-cooled substrate holder (2) where the etching temperature was maintained in range of 23 – 26 °C. The vacuum chamber of the plant UVN-2M-1 was pumped off to initial pressure values of 10^{-4} – 10^{-2} torr, whereupon plasma-forming gas was pumped in. As soon as the pressure was 20 – 25 Pa, the source (4) generating a directed off-electrode plasma flow (3) was switched on. The screen (9) with the windows 35×35 mm in size was additionally used to prevent overheating problems in the substrate holder. Such window sizes allow us to eliminate edge effects and obtain, in the substrate area, a plasma flow with regular particle distribution of at least 98% through its section. A $CF_4 + O_2$ gas at a ratio of 50:1 was used as plasma-forming gas. The parameters of the formed structure were measured with the help of a profilometer KLA Tencor P16+ and the scanning probe microscope Nano-Ink. The analysis of spectral characteristics of processed materials was performed using Raman spectroscopy by a spectrometer Nt-Mdt Ntegra Spectra with the laser emission wavelength of 532 nm.

2. Results and discussion

In response to processing in off-electrode plasma in mode of I = 80 mA and U = 2000 V, the microrelief 380 nm in depth was formed on the quartz surface. Its etching profile is given in Fig. 3.

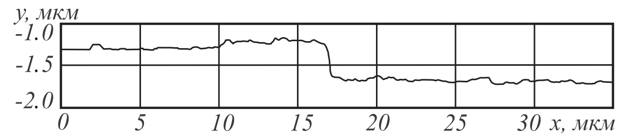

Fig. 3. Microrelief profile formed in silicon dioxide by processing a $Cr\text{-}SiO_2$ structure in off-electrode plasma

The microprofile analysis shows that the side walls have good vertical positions, since their vertical deviation does not exceed 20°. However, the surface of a groove bottom is rough; its average maximum vertical deviation is R_z = 41 nm. The analysis of a chrome film remained after having been processed by Raman spectroscopy shows the change of Raman scattering spectra as compared to chrome film spectra before irradiation (Fig. 4).

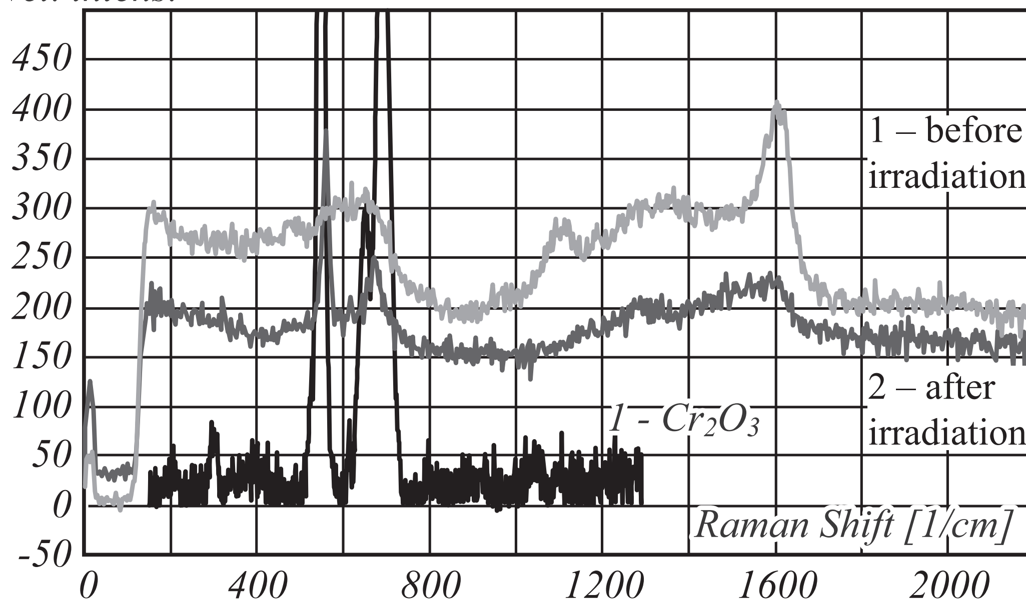

Fig. 4. Raman spectra of a thin chrome film: 1 – before irradiation, 2 – after irradiation, 3 – the spectrum of Cr_2O_3 according to data given in [16]

Several broad spectral bands with their maxima of 150, 660, 1300, 1600 cm^{-1} can be defined on spectrum of the original film (Fig. 4). A sharp, higher intensity peak with the maximum of 553 cm^{-1} is observed against the backdrop of the above maxima. The presence of broad spectral bands defines the amorphous state of the original film where there are some nanocrystallites being characterized by an intense narrow band with the maximum of 553 cm^{-1}. According to data given in paper [16], the above mentioned maximum may be referred to compounds of chromium (Cr_2O_3). The presence of chromium oxide (Cr_2O_3) is proved by the fact that the chromium films are oxidized in the course of samples

storage and transportation before lithography and etching processes.

Several broad spectral bands with their maxima of 150, 660, 1050, 1350, 1600 cm^{-1} (Fig. 4) and some thinner bands with a peak of 310, 460, 553 cm^{-1} are defined on spectrum of the processed film. Basically, the intensity of the spectral bands is increased after irradiation. Additionally, there is a slight peak displacement in the broad spectral bands towards higher values of wavenumber of 1350 and 1600 cm^{-1}. These changes of Raman spectrum characterize certain structural film transformations that result in higher crystallinity [17 – 19]. However, significant reducing in peak intensity of 553 cm^{-1} against the backdrop of the general intensity increase in the spectral bands indicates the absence of compounds of Cr_2O_3 in the processed film.

In addition, it becomes possible to allocate several additional broad spectral bands in spectra of the processed film. Their maxima correspond to the values of wavenumbers of 310, 460, 1050 cm^{-1}. Their weak maxima in the range of wavenumbers of 310, 460, 660, 1050 cm^{-1} (Fig. 4) correspond to interconnection vibrations in a space-centered cubic chrome lattice, which, according to data given in paper [20], may demonstrate Raman acoustic resonance for the values of wavenumbers of 223, 330, 460, 660, 910, 1050 cm^{-1}. The observed wide peak of 1350 cm^{-1} goes well to the wide peak in the range of wavenumber of 1344 cm^{-1}, which, according to paper [20], belongs to compounds of the formula CrO_x. The presence of a band with its peak in the range of wavenumber of 1600 cm^{-1} (Fig. 4), based on technical documentation for Raman spectroscopy data Horiba Jobin Yvon [21], confirms implementation of molecular nitrogen, having aliphatic linking N = N with maximum vibrations in the range of wavenumbers of 1550 – 1580 cm^{-1}, into the film structure.

From scientific and practical points of view, it is also important to determine the influence of etching modes in off-electrode plasma on the described properties of changing the chrome films. Resulting from varying discharge current, the behavior of Raman spectra in the processed chrome films does not change significantly. It was found that the change of spectral characteristics is linearly dependent on discharge current. Reducing of accelerating voltage to 1.2 kV has identified a remarkable thing referring to the process under consideration. It was found that plasma-chemical reaction products were deposited on the surface of silicon dioxide in the area of the rectangular chrome mask windows (Fig. 5).

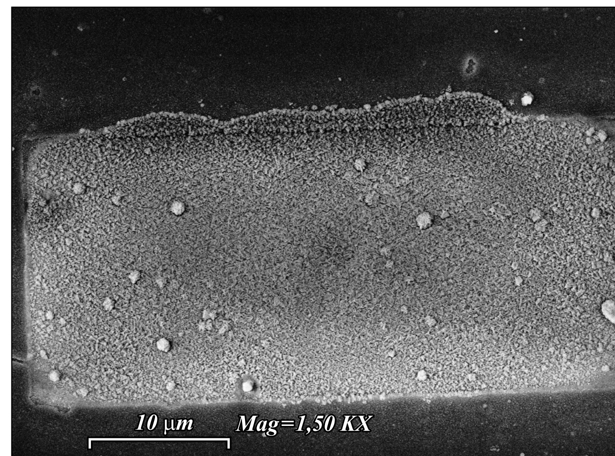

Fig. 5. Plasma-chemical reaction products deposited on the surface of silicon dioxide

The above mentioned products have the form of closely packed pyramidal crystallites shown in Fig. 6.

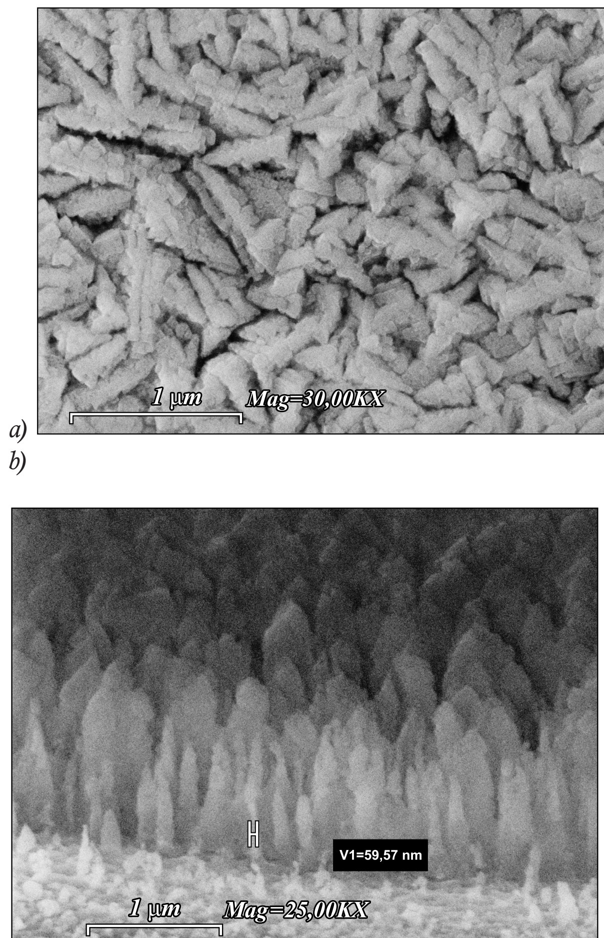

Fig. 6. Crystallites of plasma-chemical reaction products deposited on the surface of silicon dioxide: a – top view, b – side view

Besides, it can be seen in Fig. 5 that reprecipitation arises from the center of a silicon dioxide surface area towards its edges. The deposited products are "crawled" on top of the chrome mask along the long sides of the rectangular surface area, while in the corners the crystallites growth is far smaller. This configuration of the crystallites growth can be explained by peculiarities of electric field distribution generated by nonuniform discharging of the negative surface charge arising from sample surface irradiation by the directed plasma flow. In this case, the negative surface charge shall push away and/or significantly reduce the kinetic energy of electronegative plasma components. Thus, the physical spraying intensity in the area under consideration is reduced dramatically not preventing neutral and positive plasma particles to be deposited at voltage of 1.2 kV between plasma source electrodes.

At voltage of 2 kV between plasma source electrodes, reprecipitation of chrome spray products is not observed, while the chemical plasma etching process takes place. However, a high value of bottom roughness of the etched structure (Fig. 2) indirectly confirms an assumption on the described deposition mechanisms for chemical plasma reaction products. Raman spectrum of these products is given in Fig. 7.

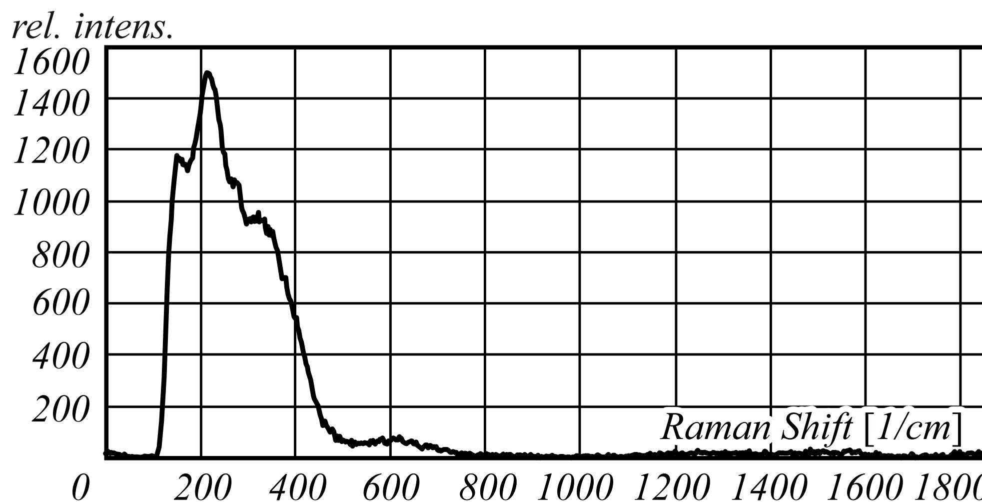

Fig. 7. Raman spectrum of plasma-chemical reaction products deposited on the surface of silicon dioxide

Typical peaks corresponding to the values of wavenumbers of 150, 225, 278, 343, 619 cm^{-1} can be selected on this spectrum.

The maximum 150 cm^{-1} is relevant to the corresponding peak on spectrum of metallic chromium. Wide bands 225, 278 confirm the presence of compounds of Cr_2N [20] in deposited products.

The maxima of wide bands of 619, 343 cm^{-1} correspond to weak maxima 615 and 350 cm^{-1} of compound of Cr_2O_3 [17].

Basically, the shape and location of spectral peaks allow us to confirm that the crystallites composition is based on compounds of the form Cr_2NO_x [16 – 20]. Formation of some larger surface globular structures (Fig. 5) is also typical for the hexagonal form of a chrome nitride lattice (Cr_2N) capable to coagulate at high temperatures.

It should be noted that in some cases spray products are also deposited at the edges of the mask windows (Fig. 8) where there is a processed metal film. In these cases, the chrome atoms serve as active centers of the crystallites growth. As can be seen from Fig. 5, this mechanism also happens to be in case, when deposited plasma-chemical reaction products are "crawled" onto the mask. At the same time, orientation of apexes and forms of the pyramidal crystallites do not change (Fig. 6b). Reprecipitation of spray products outside the mask windows might be explained by chemical plasma-assisted reactions proceeding directly on the surface of the chrome film influenced by inhomogeneities of electric fields generated in the neighborhood of silicon dioxide surface areas.

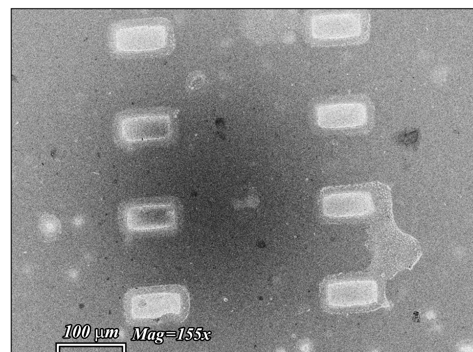

Fig. 8. Spray products deposited on the metal mask surface

Conclusion

This research has identified several peculiarities in the silicon dioxide etching process using a metal chrome mask. Resulting therefrom, it is found that the value of accelerating voltage has a great impact on etching a Cr-SiO_2 structure. Reduction of accelerating voltage to 1.2 kV results in significant decrease in the etching rate of silicon dioxide caused by plasma-chemical reaction products deposited on the surface of silicon dioxide. According to Raman spectra, a surface film of oxide is effectively removed on metal mask irradiation. In this case, off-electrode plasma does not introduce any radiation defects in a crystal lattice. On the contrary, it contributes to decreasing metal mask amorphism.

Plasma-chemical reaction products are deposited inside the metal mask windows at accelerating voltage U = 1.2 kV. Research results of Raman spectra of deposited products confirm the fact that the main component of the crystallites is a compound in the form of Cr_2NO_x. Moreover, reprecipitation of the products discussed in this paper is of considerable interest, since they are sensitive to gas-mixture composition [22]. In this case, the analysis of images of the deposited products shows that they have high values of specific free-form surface. A source of nitrogen and oxygen for forming these compounds might be adsorbed gases presenting on the surface of the chrome mask film, as well as on the walls of the vacuum chamber and technological equipment.

The obtained results allow us to clarify the silicon dioxide etching processes occurred in off-electrode plasma using the metal masks.

Acknowledgment

This work was financially supported by the grant of the President of the Russian Federation (project no. MD-5205.2016.9) and the Russian Foundation for Basic Research (grant No. 16-07-00494 A).

References

1. Bobrov ST, Greisukh GI, Turkevich YuG. Optics of diffractive elements and systems [In Russian]. Leningrad: “Mashinostroenie” Publisher, 1986.

2. Kazanskiy NL, Kolpakov VA, Kolpakov AI, Krichevsky SV. Gas-discharge devices forming directed flows of the off-electrode plasma. Part I. Analysis and structural features of devices [in Russian]. Nauchnoe Priborostroenie 2012; 22(1): 13-18.

3. Kazanskiy NL, Kolpakov VA. Study of optical microrelief formation in the plasma generated high-voltage gas discharge outside the electrode [In Russian]. Moscow: “Radio and Svyas” Publisher; 2009.

4. Kazanskiy NL, Kolpakov VA, Krichevsky SV. Simulation of cleaning the surface of the dielectric substrate in the process of plasma high-voltage gas discharge [In Russian]. Computer Optics 2005; 28: 80-86.

5. Kazanskiy NL, Kolpakov VA, Kolpakov AI. Anisotropic etching of SiO_2 in high-voltage gas-discharge plasmas. Russian Microelectronics; 2004; 33(3): 169-182. DOI: 10.1023/B:RUMI.0000026175.29416.eb.

6. Kazanskiy NL, Kolpakov VA. Effect of bulk modification of polymers in a directional low-temperature plasma flow. Tecnical phisics; 2009; 54(9): 1284-1289. DOI: 10.1134/S1063784209090060.

7. Kazanskiy NL, Kolpakov VA, Podlipnov VV. Gas discharge devices generating the directed fluxes of off-electrode plasma. Vacuum 2014; 101: 291-297. DOI: 10.1016/j.vacuum.2013.09.014.

8. Volkov AV, Moiseev OYu, Poletaev SD, Chistyakov IV. Application of thin molybdenum films in contact masks for manufacturing the micro-relief of diffractive optical elements. Computer Optics 2014; 38(4): 757-762.

9. Protasov DYu, Vitcina NR, Valicheva NA, Dulcev PhN, Malin TV, Zhuravlev KS. Chromium mask for plasma-chemical etching of Al x Ga1 x N layers. Thecnical Phisics; 2014; 59(9): 1356-1359. DOI: 10.1134/S1063784214090242.

10. Volkov AV, Volodkin BO, Dmitriyev SV, Yeropolov VA, Moiseyev OYu, Pavelyev VS. Thin film copper layer as a mask during the plasma chemical etching quartz [In Russian]. Computer Optics 2007; 31(4): 52-54.

11. Zavyalov PS, Chugui YuV. The formation of light templates for large-sized objects using the diffraction optics. Computer Optics 2013; 37(4): 419-425.

12. Veiko VP, Shakhno EA, Sinev DA. Improvement of laser thermochemical recording on thin chromium films using repeated processing [In Russian]. Izvestiya vysshikh uchebnykh zavedeniy. Priborostroyeniye 2013; 56(12): 57-61.

13. Volkov AV, Kazanskiy NL, Moiseev OY, Poletayev SD.
Thermal oxidative degradation of molybdenum films under laser ablation. Thecnical phisics 2015; 60(2): 265-269. DOI: 10.1134/S1063784215020255.

14. Nesterenko DV, Poletaev SD, Moiseev OY, Yakunenkova DM, Volkov AV, Skidanov RV. The fabrication of the curved diffraction gratings for UV [In Russian]. Proceedings of the Samara Scientific Center of the Russian Academy of Sciences 2011; 13(4): 66-71.

15. Kazanskiy NL, Kolpakov VA, Kolpakov AI, Krichevsky SV, Podlipnov VV. Gas-discharge devices forming directed flows of the off-electrode plasma. Part II. Results of updating. New devices [In Russian]. Nauchnoe Priborostroenie 2012; 22(2): 44-50.

16. He J, Lu JQ, Xie GQ, Qian L, Chen KF, Zhang XL, Luo MF. Characterization of CrOx-Y2O3 catalysts for fluorination of 2-chloro-1, 1, 1-trifluoroethane. Indian journal of chemistry. Section A 2009; 48A: 489-497.

17. Barshilia HC, Rajam KS. Raman spectroscopy studies on the thermal stability of TiN, CrN, TiAlN coatings and nano-layered TiN/CrN, TiAlN/CrN multilayer coatings. Journal of Materials Research 2004; 19(11): 3196-3205. DOI: 10.1557/JMR.2004.0444.

18. Gaisler SV, Semenova LI, Sharafutdinov RG, Kolesov BA. Analysis of the Raman spectra of amorphous-nanocrystalline silicon films. Physics of the solid state 2004; 46(8): 1528-1532. DOI: 10.1134/1.1788789.

19. Barata A, Cunha L, Moura C. Characterisation of chromium nitride films produced by PVD techniques. Thin Solid Films 2001; 398(399): 501-506. DOI: 10.1016/S0040-6090(01)01498-5.

20. Data base Project RRUFF. Eskolaite. Source: http://rruff.info/chem=Cr /notchem=Crome/display=default/R060892.

21. Raman data and analysis. Raman spectroscopy for analysis and monitoring. Source: http://www.horiba.com/fileadmin/uploads/Scientific/Documents/Raman/bands.pdf.

22. Butt N, Cinquegrani L, Mugno E, Tagliente A, Pizzini S. A family of tin-oxide-based sensors with improved selectivity to methane. Sensors and Actuators B: Chemical 1992; 6(1-3): 253-256.